HAL
open science

The signalling factor PI3K is a specific regulator of the clathrin-independent dynamin-dependent endocytosis of IL-2 receptors

Cyril Basquin, Valérie Malardé, Paul Mellor, Deborah H. Anderson, Vannary Meas Yedid, Jean-Christophe Olivo-Marin, Alice Dautry-Varsat, Nathalie Sauvonnet

To cite this version:

Cyril Basquin, Valérie Malardé, Paul Mellor, Deborah H. Anderson, Vannary Meas Yedid, et al.. The signalling factor PI3K is a specific regulator of the clathrin-independent dynamin-dependent endocytosis of IL-2 receptors. Journal of Cell Science, 2013, 126 (5), pp.1099-1108. 10.1242/jcs.110932 . pasteur-03721367

HAL Id: pasteur-03721367

https://pasteur.hal.science/pasteur-03721367v1

Submitted on 12 Jul 2022

HAL is a multi-disciplinary open access archive for the deposit and dissemination of scientific research documents, whether they are published or not. The documents may come from teaching and research institutions in France or abroad, or from public or private research centers.

L'archive ouverte pluridisciplinaire **HAL**, est destinée au dépôt et à la diffusion de documents scientifiques de niveau recherche, publiés ou non, émanant des établissements d'enseignement et de recherche français ou étrangers, des laboratoires publics ou privés.

Copyright

The signalling factor PI3K is a specific regulator of the clathrin-independent dynamin-dependent endocytosis of IL-2 receptors

Cyril Basquin[1,2], Valérie Malardé[1,2], Paul Mellor[3], Deborah H. Anderson[3], Vannary Meas-Yedid[2,4], Jean-Christophe Olivo-Marin[2,4], Alice Dautry-Varsat[1,2] and Nathalie Sauvonnet[1,2,*]

[1]Institut Pasteur, Unité de Biologie des Interactions Cellulaires, 25 rue du Docteur Roux, 75724 Paris Cedex 15, France
[2]CNRS URA 2582, 75724 Paris Cedex 15, France
[3]Cancer Research Unit, Saskatchewan Cancer Agency and Department of Biochemistry, University of Saskatchewan, 20 Campus Drive, Saskatoon, Saskatchewan S7N 4H4, Canada
[4]Institut Pasteur, Unité d'Analyse d'Images Quantitative, 25 rue du Docteur Roux, 75724 Paris Cedex 15, France
*Author for correspondence (nathalie.sauvonnet@pasteur.fr)

Accepted 10 December 2012
Journal of Cell Science 126, 1099–1108
© 2013. Published by The Company of Biologists Ltd
doi: 10.1242/jcs.110932

Summary

Receptor-mediated endocytosis is an essential process used by eukaryotic cells to internalise many molecules. Several clathrin-independent endocytic routes exist, but the molecular mechanism of each pathway remains to be uncovered. The present study focuses on a clathrin-independent dynamin-dependent pathway used by interleukin 2 receptors (IL-2R), essential players of the immune response. Ras-related C3 botulinum toxin substrate (Rac1) and its targets, the p21-activated kinases (Pak), are specific regulators of this pathway, acting on cortactin and actin polymerization. The present study reveals a dual and specific role of phosphatidylinositol 3-kinase (PI3K) in IL-2R endocytosis. Inhibition of the catalytic activity of PI3K strongly affects IL-2R endocytosis, in contrast to transferrin (Tf) uptake, a marker of the clathrin-mediated pathway. Moreover, Vav2, a GTPase exchange factor (GEF) induced upon PI3K activation, is specifically involved in IL-2R entry. The second action of PI3K is through its regulatory subunit, p85α, which binds to and recruits Rac1 during IL-2R internalisation. Indeed, the overexpression of a p85α mutant missing the Rac1 binding motif leads to the specific inhibition of IL-2R endocytosis. The inhibitory effect of this p85α mutant could be rescued by the overexpression of either Rac1 or the active form of Pak, indicating that p85α acts upstream of the Rac1-Pak cascade. Finally, biochemical and fluorescent microscopy techniques reveal an interaction between p85α, Rac1 and IL-2R that is enhanced by IL-2. In summary, our results indicate a key role of class I PI3K in IL-2R endocytosis that creates a link with IL-2 signalling.

Key words: Cytokine, Receptor-mediated endocytosis, Rac1, Signal transduction, PI3K

Introduction

Receptor-mediated endocytosis is used by eukaryotic cells to actively and specifically internalise a wide range of molecules such as nutrients or growth factors. The endocytosis process is based on the formation of inward-pointing buds that mature into vesicles, which pinch-off the plasma membrane and are carried into the cell. To date, the best-studied pathway is clathrin-dependent endocytosis, requiring the action of many well characterized factors (Mousavi et al., 2004). In this route, the receptors are recruited into clathrin-coated pits and then internalised into clathrin-coated vesicles. Several clathrin-independent pathways exist; however, their molecular mechanisms are not fully understood (Howes et al., 2010; Lajoie and Nabi, 2010; Sandvig et al., 2011). In these processes, most of the receptors are partially localized into microdomains of the plasma membrane called 'lipid rafts' (Kirkham and Parton, 2005). Some of these lipid rafts are enriched in caveolin, leading to the formation of caveolae (Nabi and Le, 2003). In addition, some cytokine receptors, such as the β chain of the interleukin 2 and 15 receptors (IL-2Rβ) and the common cytokine γ chain (IL-2Rγc) of the receptors for interleukins 2, 4, 7, 9, 15 and 21 use another endocytic route that is independent of clathrin and caveolin (Lamaze et al., 2001; Sauvonnet et al., 2005). In lymphocytes, ligand binding to these receptors induces signalling cascades leading to cell proliferation (Gaffen, 2001) and are thus essential for the immune response. These cytokine receptors can also be internalised independent of bound ligand in various cell types (Hémar et al., 1995; Subtil et al., 1997). Both constitutive and ligand-induced endocytosis of these receptors follow a clathrin-independent pathway (Subtil et al., 1994). Once internalised these receptors are sorted into lysosomes where they are degraded (Hémar et al., 1994; Hémar et al., 1995). Thus, endocytosis of cytokine receptors is a mechanism to control the signalling cascade and cell proliferation.

Some of the components of the clathrin-dependent pathway are also involved in the clathrin-independent route used by IL-2R. This is the case for the large GTPase dynamin, actin and their partners cortactin and neuronal Wiskott–Aldrich syndrome protein (N-WASP) (Engqvist-Goldstein and Drubin, 2003; Sauvonnet et al., 2005; Schmid et al., 1998; Uruno et al., 2001). In addition to these factors, our previous results have identified several specific regulators of the clathrin-independent

Journal of Cell Science

Journal of Cell Science

and dynamin-dependent pathway used by the IL-2R. The Rho GTPases, RhoA and Rac1 (Ras-related C3 botulinum toxin substrate), are specifically involved in IL-2R entry (Grassart et al., 2008; Lamaze et al., 2001). Furthermore, we identified the serine/threonine kinase, p21-activated kinase 1 (Pak1), as a downstream target of Rac1 (Grassart et al., 2008). Our data demonstrated that Pak1 phosphorylates cortactin, thereby promoting its interaction with N-WASP (Grassart et al., 2008; Grassart et al., 2010). Thus, the Rac1-Pak1 cascade upregulates the recruitment and the activation of a complex composed of cortactin, N-WASP, Arp2/3 and F-actin during IL-2R endocytosis.

The upstream regulator of the Rac1-Pak cascade still needs to be identified. A putative candidate is class I phosphatidylinositol 3-kinase (PI3K) composed of two subunits: a catalytic one (p110) and a regulatory one (p85). PI3K is a major player in the regulation of the actin cytoskeleton upon plasma membrane reorganisation. For instance, PI3K is a key player in actin recruitment during phagocytosis and macropinocytosis (Araki et al., 1996; Doherty and McMahon, 2009). However, class I PI3K has never been implicated in receptor-mediated endocytosis generating small vesicles (up to 150 nm) from the plasma membrane. By producing PI(3,4,5)P_3, PI3K induces the recruitment of several Rho GEFs including Vav proteins (Han et al., 1998). In addition, the regulatory subunit of PI3K, p85α contains a Bcr Homology (BH) domain that can bind to Rac1 (Chamberlain et al., 2004; Zheng et al., 1994), raising the possibility that p85α might act as a Rac1 recruiter. Finally, in lymphocytes producing the trimeric high affinity IL-2 receptor (α, β and γ_c chains), IL-2 binding induces the oligomerisation of the three chains and several signalling cascades such as the PI3K pathway (Gu et al., 2000). In this study we set out to test the involvement of PI3K in clathrin-independent dynamin-dependent endocytosis used by IL-2R.

Results

PI3K is specifically involved in clathrin-independent endocytosis

To investigate the role of PI3K activity we used three inhibitors of PI 3-kinase, wortmannin, LY294002 and GDC0941, a newly described inhibitor specific to class I PI3K (Folkes et al., 2008; Raynaud et al., 2009). To differentiate between constitutive and ligand-induced IL-2R endocytosis, the IL-2R-expressing human T cell line (Kit225) was used to monitor the kinetics of IL-2Rβ endocytosis in the absence or presence of IL-2, respectively.

In addition, we analysed the kinetics of transferrin (Tf) receptor (TfR) entry as a marker of clathrin-mediated endocytosis. To do this, Kit225 cells were pretreated with 25 μM LY294002, 10 μM of GDC0941 (a sufficient concentration to inhibit class I PI3K, supplementary material Fig. S1A), or DMSO and then surface labelled with a monoclonal antibody directed against the extracellular domain of the IL-2Rβ (Subtil et al., 1994) or the extracellular part of the TfR (Weissman et al., 1986). After washing, 200 pM of IL-2 were added or not, and the cells were allowed to internalise the receptors and bound antibodies at 37℃ for different times. The non-internalised receptors remaining on the cell surface were quantified by incubating cells at 4℃ with a secondary anti-mouse antibody coupled to Alexa Fluor 488 using fluorescence-activated cell sorting (FACS) analyses. Fig. 1A shows that the inhibition of PI3K does not affect the uptake of the TfR. In contrast, constitutive and IL-2-induced IL-2Rβ endocytosis were both strongly reduced in LY294002 or GDC0941 treated cells compared to the DMSO treated cells (80% and 55% inhibition respectively). The kinetics of IL-2Rβ uptake is faster in the presence of IL-2, as previously reported (Hémar et al., 1994). So in T cells, constitutive and ligand-induced IL-2R endocytosis involves PI3K activity, in contrast to TfR uptake. To confirm the requirement of PI3K activity in another cell type, we analysed the constitutive endocytosis of IL-2R in Hep2β cells, a human epithelial cell line stably expressing IL-2Rβ (Grassart et al., 2008). Cells were pretreated or not with 0.1 μM wortmannin or with 10 μM of GDC0941 and IL-2Rβ endocytosis was analysed by quantifying the uptake of an antibody against IL-2Rβ (anti-IL-2Rβ) coupled to Cy3 fluorochrome (Grassart et al., 2008) (Fig. 1B; supplementary material Fig. S1B). Clathrin-dependent entry was followed by measuring the uptake of Tf coupled to an Alexa Fluor 488 fluorochrome (TfA488, Fig. 1B; supplementary material Fig. S1C). Endocytosis of IL-2Rβ and Tf was observed with an Apotome fluorescent microscope and quantified using ICY software as previously described (de Chaumont et al., 2012; Dufour et al., 2008; Grassart et al., 2010) that automatically counts the number of vesicles and their fluorescence intensity. Quantification of the data showed that wortmannin and GDC0941 inhibited IL-2Rβ entry by 70% and 55%, respectively, compared to DMSO treated cells. In contrast, Tf uptake was not affected (Fig. 1B; supplementary material Fig. S1B,C). Therefore, PI3K activity is required for IL-2R internalisation in multiple cell types.

To reinforce the involvement of class I PI3K, we knocked down its regulatory subunit p85α by transfecting Hep2β cells with small interfering RNA (siRNA) targeting p85α or a non-targeting control siRNA. The depletion of p85α was verified and quantified by immunoprecipitation of the protein and western blots (Fig. 1C). IL-2Rβ and Tf internalisation were then monitored as described in Fig. 1B. Fig. 1D shows clearly that p85α knockdown led to the inhibition of IL-2Rβ entry by about 70% (Fig. 1E). In contrast, Tf uptake was not affected (Fig. 1D,E). To confirm the role of PI3K activity in IL-2R endocytosis, we used a mutant of p85 deleted within the p110-binding domain such that it no longer binds p110 (p85Δ110) (Chagpar et al., 2010). Overexpression of p85Δ110 inhibited IL-2Rβ endocytosis (60% inhibition) whereas Tf uptake was not affected (Fig. 1F). Therefore, class I PI3K is a new specific regulator of IL-2R endocytosis.

As PI3K has been involved in macropinocytosis, we asked whether IL-2R could enter by a macropinocytic process. We performed an endocytic assay using anti-IL-2Rβ coupled to Alexa Fluor 647, TfA488 and 500 kDa dextran coupled to rhodamine, a bona fide marker of macropinocytosis (Le Roux et al., 2012). After 15 min of endocytosis, we could see all three cargoes entering cells and no co-localisation was observed between IL-2R and dextran (supplementary material Fig. S2A). To reinforce this result, we tested the involvement of dynamin2 in IL-2R entry compared to dextran uptake. Indeed, the majority of macropinocytosis pathways are dynamin-independent (Doherty and McMahon, 2009). We transfected Hep2β cells with either green fluorescent protein (GFP)-tagged dynamin2 wild type (GFP–Dyn2WT) or a dominant-negative mutant (GFP–Dyn2K44A). We observed a strong inhibition of constitutive IL-2R internalisation in GFP–Dyn2K44A-expressing cells compared to GFP–Dyn2WT-expressing cells, as expected (supplementary material Fig. S2B). In contrast, the dominant-negative mutant of

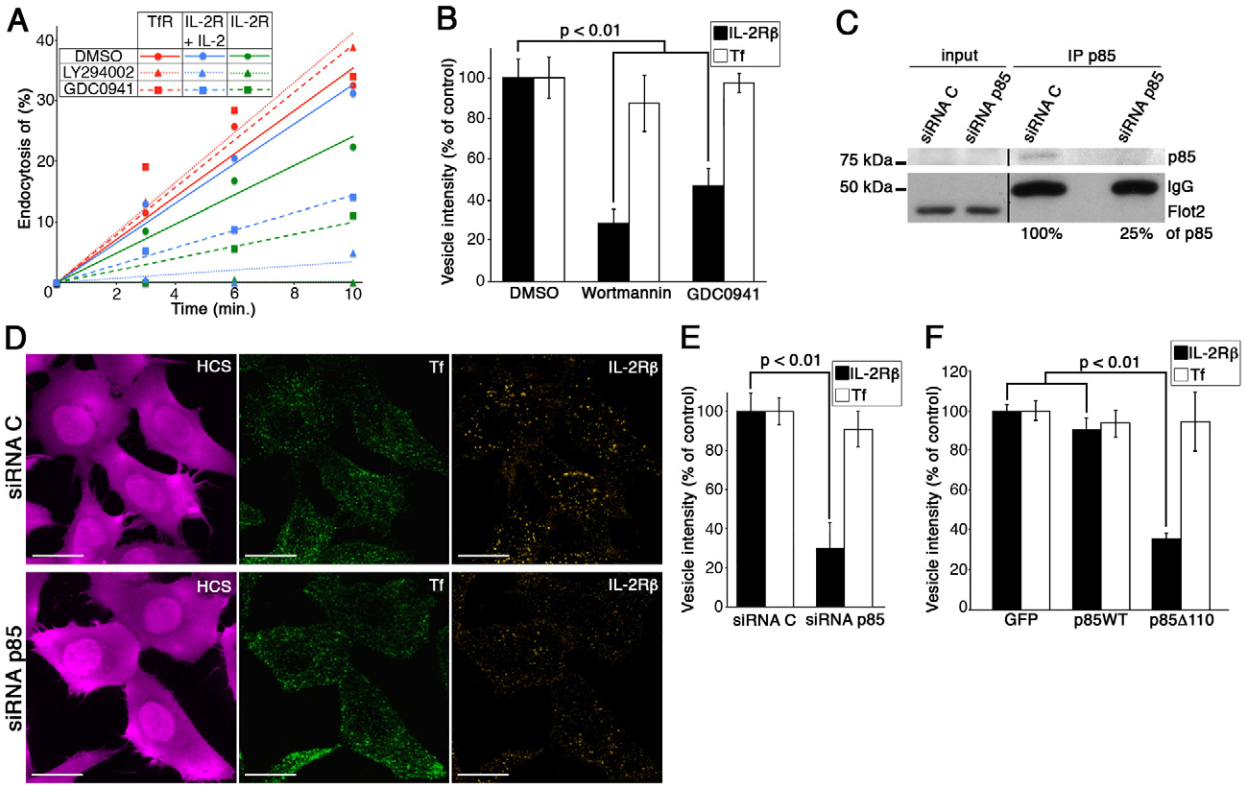

Fig. 1. PI3K is involved in IL-2R endocytosis. (**A**) T cells (Kit225) were pretreated with PI3K inhibitors, 25 μM LY294002 or 10 μM GDC0941, or with DMSO as a control. TfR and IL-2Rβ were surface labelled at 4℃ with antibodies against the receptors. Cells were incubated at 37℃ to allow constitutive endocytosis of either TfR or IL-2Rβ and induced endocytosis of IL-2Rβ by the addition of IL-2. Endocytosis was stopped at different time points and secondary antibodies coupled to Alexa Fluor 488 were used to label the surface receptors. The receptors remaining at the cell surface over time were analysed by FACS in order to quantify endocytosis. (**B**) Hep2β cells were pretreated with 0.1 μM wortmannin or 10 μM GDC0941, or with DMSO as a control. Endocytosis was monitored by incubating cells with Tf coupled to Alexa Fluor 488 (TfA488) and with an anti-IL2Rβ coupled to Cy3 (anti-IL-2Rβ–Cy3) for 15 min at 37℃. Cells were fixed and stained with HCS Cell Mask to detect cell boundaries. Quantification of endocytosis was carried out by measuring the number and fluorescence intensity of vesicles (vesicle intensity) per cell with ICY software (mean±s.d.; n>100 cells in three independent experiments, unpaired t-test). The results are expressed as a percentage of the control cells. (**C–E**) Hep2β cells were transfected either with an siRNA against the PI3K regulatory subunit p85α (siRNA p85) or with a control siRNA (siRNA C). (C) Western blots of immunoprecipitated (IP) p85α from siRNA treated cells were analysed with antibodies against p85α and with flotillin 2 (Flot2) as a control, and p85α was quantified using ImageJ and normalised to the Flot2 levels. An endocytosis assay by immunofluorescence (D) and quantification (E) were performed as described in B. A medial section is shown (D). Scale bars: 20 μm. (**F**) Hep2β cells were transfected with the FLAG-tagged wild-type form of p85α (p85WT), a mutant of p85α unable to interact with the PI3K catalytic subunit p110 (p85Δ110) or with GFP as a control. An endocytosis assay and quantification were performed as described in B using Tf coupled to Alexa Fluor 647 (TfA647) and anti-IL-2Rβ–Cy3. p85α transfected cells were identified for quantification using an anti-FLAG antibody.

dynamin2 did not affect the internalisation of dextran (supplementary material Fig. S2B), suggesting, IL-2R is not being internalised by macropinocytosis. To show that both PI3K and dynamin2 were required for IL-2R endocytosis, we verified that the strong inhibition of constitutive IL-2R entry in GFP–Dyn2K44A-expressing cells was not enhanced by the PI3K inhibitor GDC0941 (supplementary material Fig. S2C). Altogether these data demonstrate that class I PI3K is a new specific factor of the clathrin-independent dynamin-dependent endocytosis machinery used by cytokine receptors.

The Rho GEF Vav2 is specifically involved in clathrin-independent endocytosis

PI3K activation leads to the production of PI(3,4,5)P_3 subsequently recruiting several Rho GEFs. Among these GEFs, Vav family proteins are known to activate Rac1 (Abe et al., 2000; Han et al., 1998). To test the involvement of the ubiquitously expressed Vav2 protein, we knocked down its expression in Hep2β cells using specific siRNA and observed IL-2Rβ and Tf endocytosis as explained in Fig. 1B. Although the depletion of Vav2 was not total (70% depletion, Fig. 2B), we observed about 50% inhibition of constitutive IL-2Rβ endocytosis compared to cells transfected with a control siRNA (Fig. 2A,C). In contrast, Tf internalisation was not affected by Vav2 depletion (Fig. 2A,C). These data demonstrate that Vav2 is another specific regulator implicated in clathrin-independent dynamin-dependent entry used by IL-2R.

p85 acts upstream of the Rac1-Pak cascade during IL-2R entry

In addition to its role in Rac1 activation, PI3K could act via its regulatory subunit p85α, as a recruiter of Rac1. Indeed, the Bcr Homology (BH) domain of p85α was shown to interact with several small G proteins (Kang et al., 2002; Tolias et al., 1995). We first tested if the p85α BH domain was necessary for IL-2R entry. To do this, Hep2β cells were transfected with either a

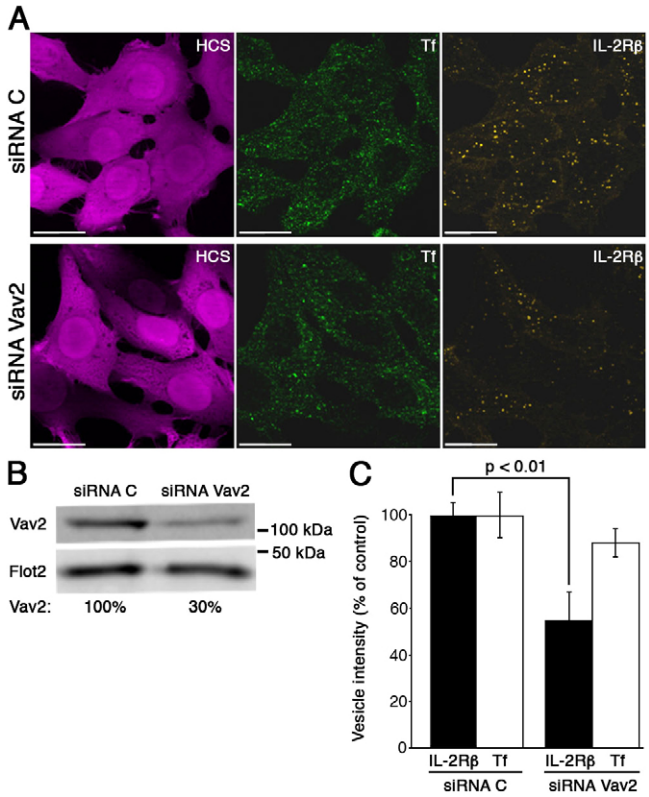

Fig. 2. The RhoGEF Vav2 is involved in IL-2Rβ endocytosis. Hep2β cells transfected either with an siRNA against Vav2 (siRNA Vav2) or with an siRNA control (siRNA C) were analysed for Tf and IL-2Rβ endocytosis as described in Fig. 1B. (**A**) A medial section is shown. Scale bars: 20 µm. (**B**) Western blots of siRNA-transfected cells were probed with antibodies against Vav2 and flotillin 2 (Flot2) as a loading control; quantification was by Storm FluoroImager and ImageQuant software. (**C**) Quantification was carried out as described in Fig. 1B using ICY software.

mutated form of p85α deleted for this domain (p85ΔBH) (Chamberlain et al., 2004) or the wild-type form as a control (p85WT), then clathrin-dependent (Tf) and -independent (IL-2R) endocytosis were analysed as explained in Fig. 1B. The overexpression of p85ΔBH inhibited IL-2Rβ endocytosis (about 50% inhibition) as compared to the overexpression of p85WT, whereas no effect was seen on Tf entry (Fig. 3A). Thus, the BH domain of p85α is important only for clathrin-independent uptake used by IL-2R.

We next tested whether the p85α BH domain was acting upstream of the Rac1-Pak cascade. For this, we attempted to rescue the inhibitory effect of the p85ΔBH mutant through overexpression of either Rac1 (GFP–Rac1), the active form of Pak1 [haemagglutinin (HA)–Pak1TE] or N-WASP (GFP–N-WASP), a downstream factor of the cascade (Grassart et al., 2008; Grassart et al., 2010). As a control, we co-overexpressed p85ΔBH and GFP and we observed around 50% inhibition of IL-2Rβ endocytosis (Fig. 3A,B). Strikingly, IL-2Rβ uptake was recovered in p85ΔBH-expressing cells when GFP–Rac1, HA–Pak1TE or GFP–N-WASP were co-expressed (Fig. 3A,B). Noteworthy, the overexpression of GFP–Rac1, HA–Pak1TE or GFP–N-WASP alone did not increase IL-2R endocytosis (supplementary material Fig. S3). These data indicate that the function of the BH domain of p85α is upstream of the Rac1-Pak cascade in IL-2R internalisation.

p85α associates with Rac1 and the IL-2R

Since the p85α BH domain can bind to small G proteins (Kang et al., 2002; Tolias et al., 1995) and acts upstream of Rac1 during IL-2R entry, we investigated the role of p85α as a Rac1 recruiter. First, we attempted to detect an association between p85α and Rac1. To do so, we constructed a glutathione S-transferase (GST)–p85α chimera, purified the protein and incubated it with immunoprecipitated GFP–Rac1 protein obtained from a Hep2β cell lysate. We observed an association between GST–p85α and

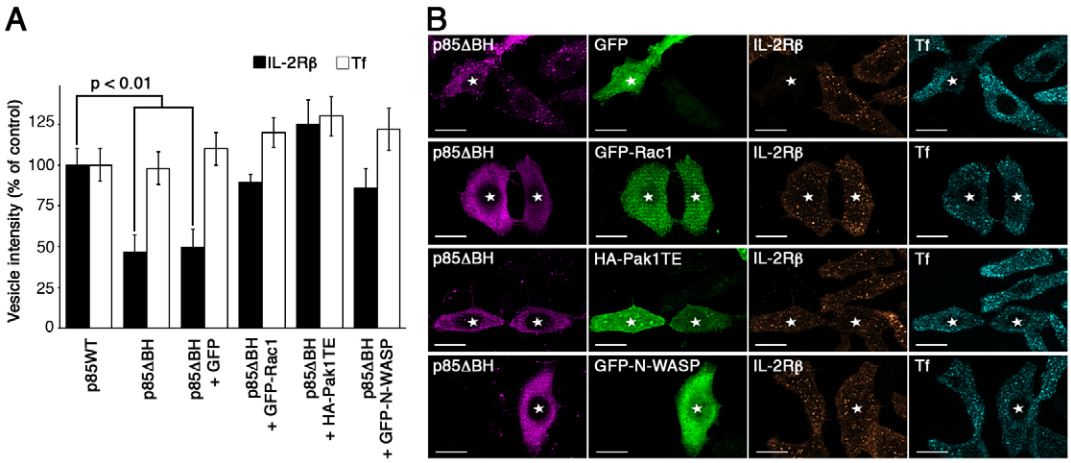

Fig. 3. p85α acts upstream of the Rac1-Pak cascade in IL-2Rβ entry. (**A**) Hep2β cells were transfected either with the FLAG-tagged wild-type form of p85α (p85WT), with a mutant of p85α devoid of its BH domain (p85ΔBH), or co-transfected with p85ΔBH and one of GFP, GFP–Rac1, the active form of Pak1 (HA–Pak1TE) or GFP–N-WASP. Endocytosis of Tf and IL-2Rβ were monitored by immunofluorescence, and quantification was carried out as described in Fig. 1F. p85α transfected cells were detected using an anti-FLAG antibody, and Pak1 transfected cells were identified with an anti-HA antibody. (**B**) A medial section of the co-transfected cells (labelled with a star) described in A is shown. Scale bars: 20 µm.

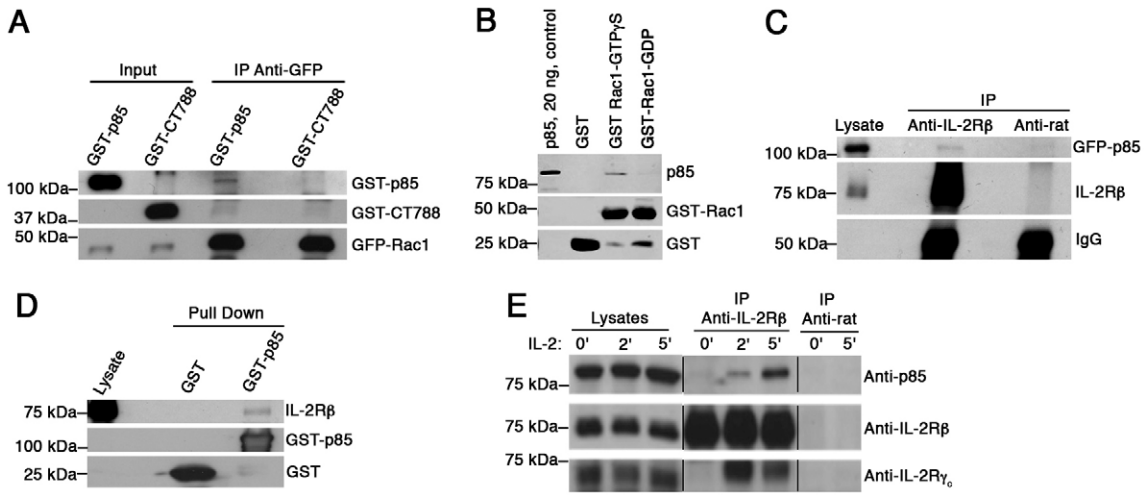

Fig. 4. p85α interacts with IL-2Rβ and Rac1. (**A**) GFP–Rac1 was recovered by anti-GFP immunoprecipitation from a lysate of Hep2β cells transfected with GFP–Rac1, incubated either with GST–p85α or with an irrelevant protein fused to GST (GST–CT788) (input), washed and eluted (IP). Western blots were probed with antibodies against GST and Rac1. (**B**) A 5 µg amount of GST or GST–Rac1 was immobilized on glutathione Sepharose beads and then the indicated nucleotide (200 µM) was loaded. Samples were incubated with purified human p85 protein, and bound protein was detected using western blots probed with antibodies against p85 and GST. (**C**) Lysates of Hep2β cells transfected with GFP–p85α were immunoprecipitated either with an antibody against IL-2Rβ or with an anti-rat IgG antibody as a control. Western blots were probed with antibodies against p85α or IL-2Rβ. (**D**) Lysates of Hep2β cells were incubated with immobilized GST–p85α or GST as a control. Western blots were probed with antibodies against GST or IL-2Rβ. (**E**) Starved Kit225 cells were incubated with 200 pM IL-2 for 2 or 5 min, lysed, and endogenous IL-2Rβ was immunoprecipitated using anti-IL-2Rβ or anti-rat IgG as a control. Bound proteins were detected by probing western blots with the indicated antibodies.

GFP–Rac1 (Fig. 4A). As expected an irrelevant GST chimera, named GST–CT788, did not associate with GFP–Rac1 (Fig. 4A). Thus, as expected, p85α interacts with Rac1. To determine which form of Rac1 (GTP or GDP bound) was interacting with p85α, we performed an *in vitro* pull-down assay as previously described (Chamberlain and Anderson, 2005). Fig. 4B shows that p85α binds directly to Rac1 and more efficiently to Rac1–GTP than to Rac1–GDP. This result suggests that Rac1 is first activated and then recruited by p85α.

To determine an association between p85α and IL-2Rβ, we constructed a GFP–p85α fusion and transfected it into Hep2β cells. Immunoprecipitation experiments using IL-2Rβ antibodies showed that GFP–p85α could be co-immunoprecipitated with IL-2Rβ (Fig. 4C). The reverse pull-down assay using GST–p85α was done and showed an association between GST–p85α and IL-2Rβ (Fig. 4D). Thus in Hep2β cells we observe an association of IL-2Rβ with p85α. We then tested if this interaction was occurring in lymphocytes and whether it was enhanced by IL-2 treatment. We attempted to observe a co-immunoprecipitation of endogenous IL-2Rβ with p85α in Kit225 cells treated or not with IL-2 (Fig. 4E). We could detect a small amount of co-immunoprecipitation of p85α with IL-2Rβ in Kit225 not treated with IL-2 (Fig. 4E). When cells were treated with IL-2 for 2 or 5 min, we observed an increased level of co-immunoprecipitation of p85α with IL-2Rβ (Fig. 4E). Addition of IL-2 to Kit225 cells for 2 min is sufficient to induce the oligomerisation of the trimeric receptor as seen by the co-immunoprecipitation of IL-2Rβ with IL-2Rγc (Fig. 4E). Thus, our data demonstrate that in lymphocytes p85α is associated with endogenous IL-2Rβ and IL-2 stimulation enhances this association.

To determine whether the p85–IL-2Rβ interaction occurred during endocytosis, we tested if these two proteins were co-localized at the plasma membrane surface by using total internal reflection fluorescence (TIRF) microscopy. This technique restricts the observations to the first 100–200 nm from the coverslip, allowing the visualisation of events taking place at the plasma membrane but not those from internalised proteins (Fish, 2009). We performed TIRF acquisitions in live Hep2β cells transfected with GFP–p85α and observed GFP–p85α and IL-2Rβ simultaneously using anti-IL-2Rβ coupled to Cy3. As a control, live TIRF imaging was performed to observe Tf coupled to Cy3 (Tf–Cy3) and GFP–p85α simultaneously. Each movie was then analysed using ICY software adapted to TIRF image analysis, allowing an automatic detection of GFP–p85α, anti-IL-2Rβ–Cy3 or Tf–Cy3 over time (Fig. 5A). The co-localization analyses were carried out for each movie and statistical relevance calculated (Fig. 5A,B). The analysis from six movies showed that around 15% of GFP–p85α co-localized with IL-2Rβ (Fig. 5A,B). Moreover, these p85α and IL-2R spots remained co-localized for about 7 seconds. In contrast, GFP–p85α was never seen co-localized with Tf (Fig. 5A,B). Our results show a specific interaction of p85α with IL-2Rβ at the plasma membrane. Altogether, our data demonstrate that the regulatory subunit of PI3K p85α interacts with both Rac1 and IL-2Rβ during clathrin-independent endocytosis.

PI(3,4,5)P_3 is involved in clathrin-independent endocytosis

Class I PI3K phosphorylates PI(4,5)P_2 on the D3 position, generating PI(3,4,5)P_3. Our data, especially on Vav2 and TIRF microscopy, strongly suggest that PI(3,4,5)P_3 is the PI3K product involved in IL-2R entry. To strengthen this hypothesis, we attempted to reduce the level of PI(3,4,5)P_3 and then tested the effect on IL-2R endocytosis. For this we used two constructs depleting intracellular levels of PI(4,5)P_2 and PI(3,4,5)P_3 (Malecz et al., 2000): the PI5-phosphatase synaptojanin 2 (SJ2) and a chimera bearing the phosphatase domain of SJ2 targeted to the membrane through a CAAX domain (PD-CAAX). The overexpression of SJ2 or PD-CAAX inhibited constitutive IL-2R

Journal of Cell Science

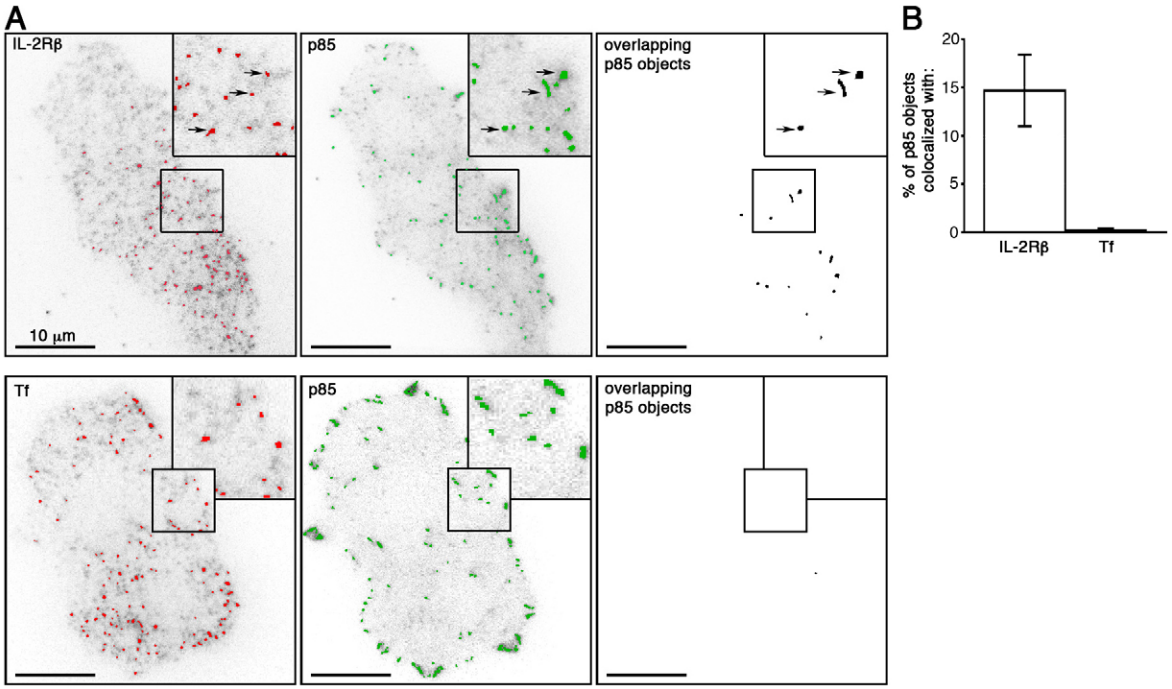

Fig. 5. p85α and IL-2Rβ co-localize at the plasma membrane. (**A**) TIRF images of Hep2β cells transfected with GFP–p85α and incubated with either Tf–Cy3 or anti-IL-2Rβ–Cy3 were obtained from a movie of 100 seconds at 1 Hz. p85α (green), Tf (red) and IL-2Rβ (red) objects were detected by ICY software and overlaid on TIRF images. Co-localized objects were identified (right-hand panel) and quantified by ICY software (**B**) (mean±s.d.; n=5 movies for Tf, n=6 movies for IL-2Rβ). Insets represent a 2-fold magnification.

endocytosis as well as Tf uptake as previously described (Malecz et al., 2000) (supplementary material Fig. S4). This strongly suggests that PI(3,4,5)P_3 is the lipid required for IL-2R endocytosis. To reinforce this result, we compared, the co-localization of IL-2R with a chimera commonly used to detect PI(3,4,5)P_3, composed of a GFP tag and the PH domain of Akt (GFP–PHAkt). GFP–PHAkt-transfected cells preincubated with DMSO or GDC0941 were incubated with anti-IL-2R–Cy3 and TfA647 for 5 min at 37℃ to allow the labelling of both surface and endosomal receptors. GFP–PHAkt was associated with the plasma membrane in DMSO-treated cells, in contrast to GDC0941 treated cells where GFP–PHAkt was mostly cytosolic (Fig. 6A). This confirms that GDC0941 inactivates class I PI3K and that GFP–PHAkt is a bona fide PI(3,4,5)P_3 marker. IL-2R was seen predominantly associated with membrane protrusions enriched in GFP–PHAkt in DMSO treated cells and not in GDC0941 treated cells (Fig. 6A). In contrast Tf was not seen associated with GFP–PHAkt at the plasma membrane. Furthermore, we tested the recruitment of Vav2 at the plasma membrane in the presence or absence of the PI3K inhibitor wortmannin. In DMSO-treated cells, GFP–Vav2 was at the plasma membrane enriched in membrane protrusions where IL-2R could be seen (Fig. 6B). In contrast, GFP–Vav2 was mainly cytosolic when PI3K was inhibited and not associated to IL-2R (Fig. 6B). Therefore, our data indicate that PI(3,4,5)P_3 is the required lipid necessary for clathrin-independent but dynamin-dependent endocytosis of the IL-2R.

Discussion

We identify for the first time that PI3K as a key player in receptor-mediated endocytosis of the IL-2R. In particular our work shows that class I PI3K is specifically involved in clathrin-independent but dynamin-dependent endocytosis of IL-2Rβ by regulating the Rho GTPase Rac1. Our data reveal that PI3K has two actions mediated by its catalytic activity and its regulatory factor p85α. Indeed, we identified that the RhoGEF Vav2, induced by PI(3,4,5)P_3 production, is involved in IL-2Rβ internalisation. Moreover, our results show that p85α, by interacting with IL-2Rβ, can act as a recruiter of Rac1–GTP during endocytosis. Thus, we propose a working model whereby p85α interacting with IL-2Rβ activates PI3K activity leading to the production of PI(3,4,5)P_3 and the induction of Vav2, the GEF to activate Rac1 (Fig. 7). Activated Rac1–GTP would be then recruited to sites containing the IL-2R via its direct binding to p85α. Finally, this would activate the Rac1-Pak1-N-WASP cascade and enhances the rate of actin polymerization during clathrin-independent endocytosis of IL-2Rβ (Fig. 7).

Our results indicate the specific involvement of Vav2 in IL-2Rβ entry; however, we observed only a 50% inhibition of endocytosis when Vav2 was depleted (Fig. 2). This partial effect of Vav2 depletion may be due to an incomplete depletion of Vav2. Indeed, although we used several siRNAs targeting Vav2, we never obtained more than 70% Vav2 depletion. Vav2 belongs to a Rho GEF family comprising three members: Vav1, Vav2 and Vav3, which might have redundant actions. Alternatively, another Rho GEF could be also responsible for Rac1 activation during IL-2Rβ endocytosis.

Our data reveal a new role for p85α as a Rac1 recruiter during IL-2Rβ endocytosis. Several lines of evidence allowed us to conclude this function for p85α. First, our results show that p85α could bind directly to Rac1–GTP (Fig. 4B), in agreement with previous reports (Kang et al., 2002; Tolias et al., 1995). Second,

Journal of Cell Science

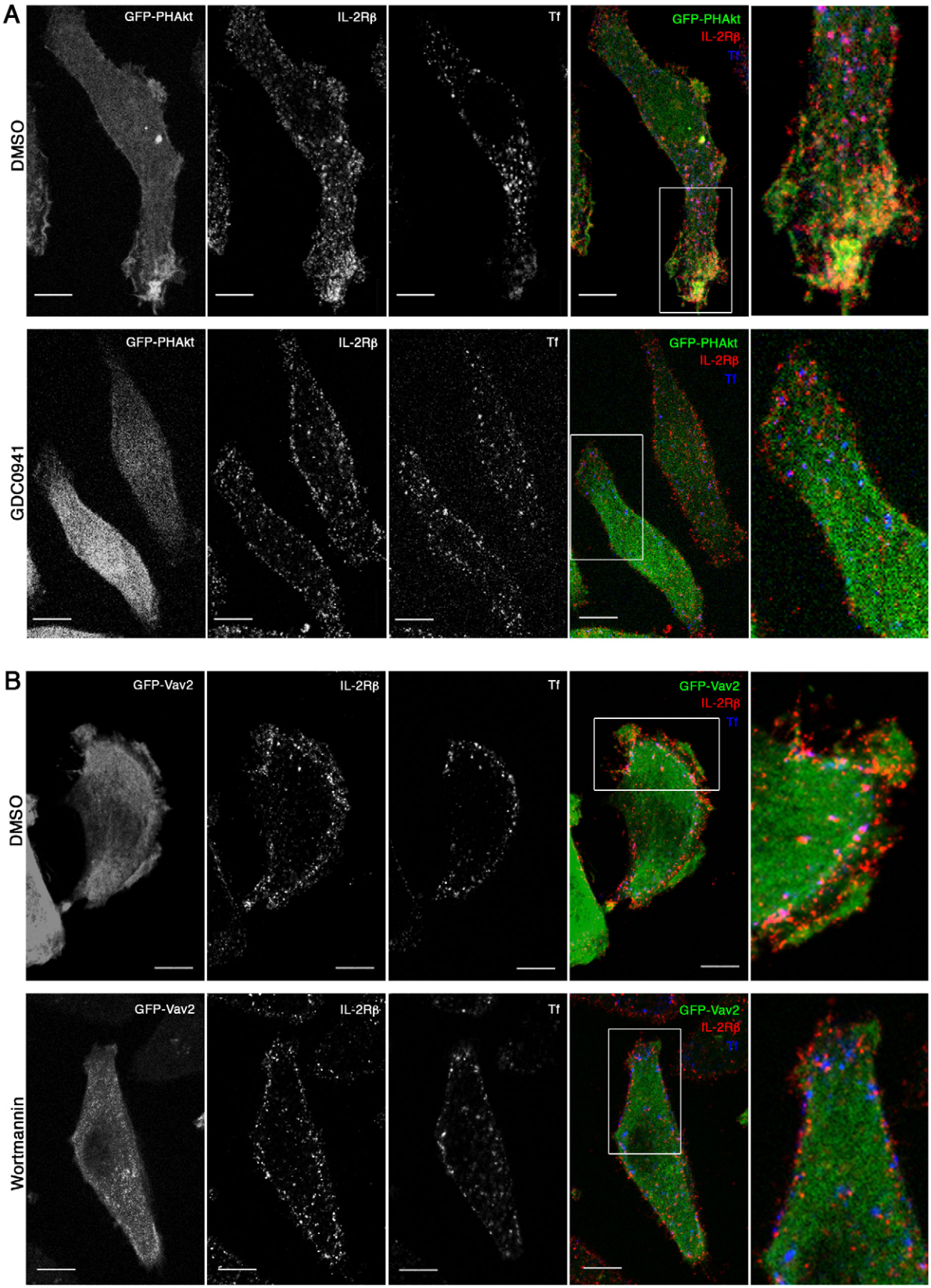

Fig. 6. PI(3,4,5)P_3 is involved in IL-2R endocytosis. (**A**) Hep2β cells transfected with a PI(3,4,5)P_3-binding protein, the PH domain of Akt tagged with GFP (GFP–PHAkt), were pretreated with 10 μM GDC0941 or DMSO as a control. Cells were incubated for 5 min at 37℃ with TfA647 (blue) and anti-IL-2R–Cy3 (red). A medial section is shown. Scale bars: 10 μm. Panels to the right represent a 2.5 fold magnification of the merge inset. (**B**) Hep2β cells transfected with GFP–Vav2 were treated as described in A except that cells were pretreated with 0.1 μM wortmannin instead of GDC0941.

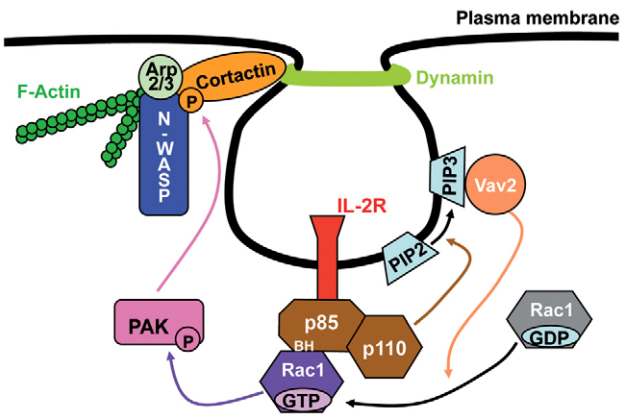

Fig. 7. Working model for clathrin-independent IL-2R endocytosis. IL-2Rβ in association with p85α would activate PI3K, leading to the induction of Vav2 and the activation of Rac1. Activated Rac1 would be then recruited to IL-2R via its association with p85α. This in turn would induce the Rac1-Pak1-N-WASP cascade and actin polymerization during endocytosis.

the BH domain of p85α, previously shown to bind Rac1, was necessary for IL-2Rβ endocytosis (Fig. 3A). Third, our rescue experiments (Fig. 3A,B) demonstrated that the function of p85α in IL-2Rβ internalisation was upstream of the Rac1-Pak cascade. Altogether these data suggest a model where p85α function is linked to the recruitment of Rac1.

The association of p85α with IL-2Rβ further strengthens the role for p85α as a Rac1 recruiter. Endogenous p85α co-immunoprecipitated with IL-2Rβ in lymphocytes and an *in vitro* pull-down assay using GST–p85 confirmed its interaction with IL-2Rβ (Fig. 4C,D,E). In addition, these results are in agreement with the co-localization observed using TIRF microscopy and ICY software (Fig. 5A,B). Indeed, our results show that at the plasma membrane 15% of p85α is co-localized with IL-2Rβ for about 7 seconds. This indicates that this interaction is transient. Recently, the dynamics of recruitment of factors involved in clathrin-mediated endocytosis was investigated using live TIRF imaging and some important factors such as dynamin were seen very transiently recruited to clathrin-coated pits (Taylor et al., 2011). The transient interaction of p85α with IL-2Rβ then allows the recruitment of Rac1 and the activation of actin polymerization during endocytosis.

Class I PI3K is clearly involved in phagocytosis and macropinocytosis (Doherty and McMahon, 2009; Huynh and Grinstein, 2008). Both mechanisms require profound reorganization of the actin cytoskeleton to generate large vesicles. In these cases, PI3K triggers the activation of Rac1 and actin polymerization (Doherty and McMahon, 2009; Huynh and Grinstein, 2008). However, the precise mechanism by which PI3K induces Rac1 has not been clearly defined. Interestingly, during macropinocytosis, Rac1 leads to the induction of the kinase Pak1 (Dharmawardhane et al., 2000). Therefore, it appears that IL-2R endocytosis and macropinocytosis are closely related. However, the size of the vesicles generated, the absolute requirement of dynamin for IL-2R endocytosis and the absence of co-localization between IL-2R and dextran allows us to discriminate between the two pathways (supplementary material Fig. S2). Nevertheless, it would be interesting to test whether p85α can act as a Rac1 recruiter in macropinocytosis and phagocytosis. In addition to its role in the creation of large vesicles, class I PI3K activity was also involved in Glut4 and GPCR trafficking (Antonescu et al., 2009; Dalle et al., 2002), but the role of this kinase in endocytosis was not further investigated.

Lastly we observed that PI3K is involved in both constitutive and IL-2-induced endocytosis of the IL-2Rβ (Fig. 1A,B). In lymphocytes expressing the trimeric IL-2 receptor (α, β and γ_c chains), IL-2Rβ can be internalised with or without the ligand. However, the kinetics of internalisation are faster in the presence of IL-2 (Fig. 1A) (Hémar et al., 1994). It was previously proposed that the signalling cascade induced by IL-2 could increase endocytosis (Gesbert et al., 2004). Although IL-2Rβ or γ_c chains have no intrinsic kinase activity, IL-2 induces the PI3K pathway, thereby participating in lymphocyte proliferation (Gesbert et al., 2004). Consistently we observed that IL-2 enhances p85α–IL-2R association in lymphocytes. Since class I PI3K is involved in IL-2R endocytosis, its enhanced association in the presence of IL-2 might contribute to the faster IL-2R internalisation observed when IL-2 is present. As IL-2Rβ and γ_c are then sorted to lysosomes where they are degraded (Hémar et al., 1995), endocytosis is a way to control signalling cascades induced by cytokines. Our present work indicates that besides its important role in IL-2 signalling, PI3K allows better control of cell proliferation by contributing to IL-2Rβ endocytosis.

Materials and Methods

Cells, constructs and reagents

The human T cell line Kit225 was maintained in RPMI containing 10% FCS and 200 pM IL-2 (a gift from A. Minty, Sanofi-Synthélabo, Labege, France). Hep2β cells (Grassart et al., 2008) were grown in DMEM containing 10% FCS and 1 mg/ml of geneticin (Gibco). GFP–N-WASP, GFP–Rac1, HA–Pak1TE, GFP–PHAkt, GFP–Dyn2Wt, GFP–Dyn2K44A, myc–SJ2, myc–PD-CAAX and GFP–Vav2 constructs were generous gifts from Drs B. Qualmann (Kessels and Qualmann, 2002), E. Caron (Patel et al., 2002), J. Chernoff (Sells et al., 1997), P. Chavrier, M. McNiven (Baldassarre et al., 2003; Cao et al., 1998), M. Symons (Malecz et al., 2000) and L. Buday (Tamás et al., 2003), respectively. The GST–p85 plasmid was generated as follows. Total RNA was isolated from HEK293 cells using the RNeasy kit (Qiagen) and cDNA was synthesized from the RNA using the Superscript II Reverse Transcriptase kit (Invitrogen). PCR was used to amplify full-length human p85α (amino acids 1–724) from the cDNA using primers designed to add BamH1 and EcoR1 restriction sites to either end of the sequence. Following restriction digest the full-length human p85α was ligated into pGEX6P1 (GE Healthcare). The insert sequence was verified by DNA sequencing. Mammalian expression vectors expressed triple FLAG-tagged p85 (bovine) containing the following residues: p85wt (amino acids 1–724); p85ΔBH (amino acids 1–83 and 314–724); p85Δ110 (amino acids 1–477 and 514–724) were described (Chagpar et al., 2010; Chamberlain et al., 2004; King et al., 2000).

To obtain GFP-tagged p85α, we cloned p85α from the pGEX6P1(GST)-p85α construct (restriction enzyme EcoR1/BamH1) into pEGFPc1 (Clontech) (restriction enzyme EcoR1/*Bgl*II). The PI3K inhibitors wortmannin (Calbiochem) was used at 0.1 μM, LY294002 (Calbiochem) was used at 25 μM and GDC0941 (Selleckchem) was used up to 10 μM, all were incubated on starved cells for 30 min before endocytic assays.

Transfection and siRNA experiments

Plasmid introduction was done using electroporation (300 V and 500 mF, Biorad) of 4×10^6 Hep2β cells with 10 μg of DNA for single transfection or 7 μg of both plasmids for co-transfections. After 24 h, cells were used to monitor endocytosis or immunoprecipitation experiments. Small interfering RNA (siRNA) were designed and synthesized by MWG Biotech. Sense sequences were for siRNA p85α: AUACCGUUGUUGGCUACAGUA, siRNA Vav2: GAAUGACGAUGACGUC-UACtt, Control siRNA was ON-TARGET plus control® siRNA (Thermo Scientific Dharmacon). Vav2 siRNA was introduced by electroporation of 200 pmol siRNA for 4×10^6 Hep2β cells. For siRNA p85α, 20 pmol were introduced by using Lipofectamine™ RNAiMAX (Invitrogen) in 0.5×10^5 cells. All siRNA transfected cells were analysed 72 h after transfection.

Endocytosis, immunofluorescence, FACS and microscopy

Kit225 cells were IL-2 starved, pretreated with LY294002 or GDC0941 inhibitor, incubated for 30 min at 4°C either with anti-IL-2Rβ (561) mouse antibody (Ab)

(Subtil et al., 1994) or with anti-TfR mouse Ab (OKT9) (Weissman et al., 1986) and then incubated at 37℃. It should be noted that anti-IL-2Rβ does not compete with IL-2 for binding to IL-2R. If indicated, 200 pM of IL-2 was added. At different time points, samples were transferred to 4℃ and incubated with an anti-mouse antibody coupled to AlexFluor488 for 30 min at 4℃. Analysis was performed with a FACSCalibur flow cytometer (BD Biosciences). At least 5000 cells were analysed in 3 different experiments. Results were expressed as a percentage of endocytosis over time corresponding to the decreased amount of surface receptor. Hep2β cells transfected or pretreated with wortmannin or GDC0941 were used to perform endocytosis assays as described previously (Grassart et al., 2008). Either Tf coupled to Alexa Fluor 488 (TfA488, Molecular Probes) or Tf coupled to Alexa Fluor 647 (TfA647, Amersham), anti-IL2Rβ coupled to cyanine 3 (Cy3) or to Alexa Fluor 647 (Amersham) and/or 500 kDa dextran coupled to rhodamine (1 mg/ml) (Le Roux et al., 2012) were added to the cells for a time course up to 15 min at 37℃ to allow receptor entry (Grassart et al., 2010). Cells were fixed and permeabilized as described in Grassart et al. (Grassart et al., 2008). The specific primary antibodies used were anti-HA rat Ab (Invitrogen, 1:100), anti-myc (mouse antibody 9E10, ascites 1/500) or anti-FLAGM2 mouse Ab (Sigma-Aldrich, 1:2000). The secondary antibodies were anti-rat-A488 (Molecular Probes, 1:200) and anti-mouse IgG1 coupled to Alexa Fluor 350 (Molecular Probes, 1:100). To detect cell boundaries, cells were stained with HCS Cell Mask Alexa Fluor 350 (Invitrogen Molecular Probes, 1.25 ng/ml). Fluorescence images were obtained with an Apotome fluorescent microscope (Zeiss) and a Roper Scientific Coolsnap HQ camera equipped with a 63×objective to acquire a Z series of 1 µm optical sections, a medial section was shown in figures. For quantification, images were obtained with a 20×objective under the same acquisition settings. Images collected from at least three independent experiments, representing at least 100 cells, were further analysed using ICY software.

GST–protein production and pull down assays

GST–p85 was expressed in *Escherichia coli* BL21 bacteria and grown at 37℃ until OD_{600} reached 0.4, transferred to 16℃ and 0.1 mM IPTG (Euromedex) was added at OD_{600}=0.6 to induce protein expression. Cultures were then grown for 16 h at 16℃, centrifuged and pellets were sonicated in PBS supplemented with protease inhibitor cocktail (PIC) (Sigma-Aldrich) and 1 mM PMSF to obtain lysates. Triton X-100 was added to 1% and samples were centrifuged for 30 min at 12,000 ***g*** at 4℃. Supernatants were filtered with a 0.45 µm filter, incubated with Glutathione Sepharose™ 4B (GE Healthcare), washed and either purified with an elution buffer [10 mM L-glutathione (Sigma-Aldrich), 150 mM NaCl and 50 mM Tris, pH 8] (Fig. 4A) or further incubated with lysates of Hep2β to co-precipitate IL-2Rβ (Fig. 4D). Purified GST–CT788 protein was a generous gift of Dr A. Subtil. For Fig. 4B, 5 µg GST or GST–Rac1 were immobilized on glutathione Sepharose beads. Nucleotide was removed by treatment with EDTA (10 mM), then the indicated nucleotide (200 µM) was loaded with 10 mM $MgCl_2$. Samples were blocked in 1% milk, then incubated with purified human p85 protein (5 µg/100 µl in 1% milk) for 1 hour at room temperature. Beads were washed three times and samples were eluted in 12 µl SDS sample buffer. Most of the sample (10 µl) was analyzed for bound p85 by western blotting using an anti-p85 antibody (Upstate Biotechnology Inc. cat. no. 05 212), used according to the manufacturer's instructions. An aliquot (2 µl) was also analysed for GST and GST–Rac1 input by western blotting using an anti-GST antibody (Santa Cruz Biotechnology, cat. no. sc-138, used at 0.25 µg/ml). Secondary anti-mouse-IRDye 680 antibodies (LI-COR Biosciences) were used to visualize bound antibodies with a LI-COR Odyssey scanner. Similar results were observed in all binding experiments.

Immunoprecipitation and western blotting

4×10^6 Hep2β cells transfected with siRNAs (Fig. 1C), 8×10^6 Hep2β cells transfected with plasmid (Fig. 4A,C,D) or 10×10^6 Kit225 cells pretreated or not with 200 pM of IL-2 for 2 or 5 min (Fig. 4E) were lysed in ice cold lysis buffer [50 mM Tris (pH 8), 150 mM NaCl, 10 mM NaF, 1 mM EDTA, 1 mM EGTA, 0.5% Triton X-100, 1 mM iodoacetamide, 1 mM PMSF, 1 mM sodium orthovanadate, PIC (Sigma-Aldrich)], and centrifuged for 20 min at 15,000 ***g*** at 4℃ to obtain the lysates. In Fig. 1C, lysates were incubated with protein G Sepharose 4 Fast Flow (GE Healthcare) coupled to anti-p85α mouse Ab (clone AB6, Millipore). In Fig. 4A, lysates were incubated with anti-GFP mouse antibody (4E6), washed, mixed with protein A Sepharose™ CL-4B (GE Healthcare), and further incubated with 0.27 µM of either GST–p85α or GST–CT788 as a control in a buffer (3 mM $MgCl_2$, 0.4 mM EGTA, 0.7 mM EDTA, 30 mM HEPES, pH 7.5). In Fig. 4C, lysates were incubated with anti-IL-2Rβ (C-20, Santa Cruz Biotechnology) or with anti-rat antibody (Biosys) as a control, washed and mixed with Protein A Sepharose™ CL-4B (GE Healthcare). In all experiments, after washes, bound proteins were eluted by boiling in Laemmli buffer for 5 min, loaded on SDS-PAGE and analysed by western blot (WB). For Fig. 2, 72 h after siRNAs transfections, total protein extracts from 10^5 cells were analysed. Antibodies used for WBs were anti-p85α mouse Ab (Millipore, 1:500), anti-flotillin2 mouse Ab (BD Biosciences, 1:2000) for loading control (Grassart et al., 2008), anti-vav2 rabbit Ab (Santa Cruz Biotechnology, 1:200), anti-GFP rabbit Ab (Santa Cruz Biotechnology, 1:500), anti-GST mouse Ab (1D10, Euromedex, 1:1000), anti-phospho-Akt(ser473), anti-Akt(pan) (both from Cell Signaling Technology Inc., 1:1000), anti-IL-2Rβ rabbit Ab (Santa Cruz Biotechnology, 1:1000) and anti-IL-2Rγ (BD Biosciences, 1:1000). The secondary antibodies used were the enzyme horseradish peroxidase (HRP) linked either to anti-mouse (GE Healthcare, 1:3000), or to anti-rabbit (GE Healthcare, 1:10,000) and visualised by ECL or alkaline phosphatase linked either to anti-mouse (Pierce, 1:5000) or to anti-rabbit (Pierce, 1:5000), visualised by ECF and quantified by Storm FluoroImager. For all WBs, input represents 2.5% of total lysate loaded on the gel.

TIRF microscopy

1×10^5 Hep2β cells transfected with GFP–p85α and plated on MatTek plates were starved for 30 min, then incubated 2 min with either Tf–Cy3 or anti-IL2Rβ–Cy3 in a TIRF medium (25 mM HEPES, 135 mM NaCl, 5 mM KCl, 1.8 mM $CaCl_2$, 0.4 mM $MgCl_2$, 4.5 g/l glucose, pH 7.4 and 0.5% BSA) at 37℃ and washed. Then cells were incubated in an environmental control system set to 37℃ and movies of 100 seconds at 1 Hz were acquired. Experiments were performed using a TIRF microscope (IX81F-3, Olympus) equipped with a 100×NA 1.45 Plan Apo TIRFM Objective (Olympus) and fully controlled by Cell^M (Olympus). Two solid-state laser lines (488 and 561 nm) (Olympus) were coupled to a TIRF condenser through two optical fibres. The two colour channels were simultaneously acquired through a Dual View beam splitter (Optical Insights), to separate the two emission signals to two sides of the camera, using a 565 nm dichroic mirror and 525/50 and 605/55 nm emission filters. Images were collected using an Ixon^{EM}+ Camera (DU885, Andor).

Image analysis by ICY

In order to quantify endocytic events, we have developed an automated framework composed of two principal components (1) robust cell segmentation using coupling shape-constrained active contours and (2) efficient fluorescence-labelled spots/vesicles quantification based on wavelet transform. We use an HCS cell mask, which enables the labelling of the nucleus and the cytoplasm of the cell to initiate the active contours. In the next step, the two populations (transfected versus non transfected) are automatically clustered by applying the K-means algorithm to distinguish the two populations. Then, the vesicle number and vesicle intensity per cell in each population (transfected or not) are computed and the sum of the total vesicle intensity in each population is calculated (this integrates both vesicle number and intensity). Finally, the results are expressed as a percentage of control cells. Student's *t*-test was used for statistical analysis.

All the TIRF images analyses were performed using ICY software. Images were first corrected for microscope misalignment and photobleaching. Objects were detected in both channels and overlapping objects were then identified. We defined an overlapping area of three pixels as a co-localization between two objects. We computed a coarse statistical relevance: one spot is approximated by a square and represented by its mass centre, then the image is downsampled by this approximation value and a spot is represented by a point. We defined N=detection number in channel 1, M=detection number in channel 2 and A=area of the cell. If there are K co-localizations the probability to get K couples follows a Bernouilli distribution and is expressed by $P_K = C_{NM}^K \left(\frac{1}{A}\right)^K \left(1-\frac{1}{A}\right)^{(NM-K)}$. To determine if the probability to have K co-localizations is relevant, we computed the probability to get randomly K co-localized couples by $P = \sum_{i=K}^{NM} C_{NM}^i \left(\frac{1}{A}\right)^i \left(1-\frac{1}{A}\right)^{(NM-i)}$. If this probability P is small enough (<0.05), then we concluded that having K co-localizations is not due to chance. Co-localizations were computed for 5 (Tf) or 6 (IL-2R) cells representing each time a movie of 100 images and the results were expressed as a mean percentage of co-localization (http://icy.bioimageanalysis.org).

Acknowledgements

We are most grateful to Prof. Paul Lazarow for critical reading of this manuscript. The generous gift of reagents by Drs Caron, Chavrier, Chernoff, Hall, McNiven, Niedergang, Qualmann and Dr Symons are gratefully acknowledged. We thank Annick Dujeancourt for technical help.

Author contributions

C.B. performed the experiments and participated in the writing of the manuscript; V.M. performed experiments; P.M. and D.H.A. performed experiments and corrected the manuscript; V.M.Y. and J.C.O.M. designed algorithms to quantify the data; A.D.V. corrected the manuscript and N.S. performed and designed experiments and wrote the manuscript.

Funding

This work was supported by the Conseil Pasteur-Weizmann [grant to N.S.]; and the Canadian Cancer Society Research Institute [grant to D.H.A.]. C.B. is supported by ED no. 426 'Gènes, Génomes, Cellules' and 'La Ligue Contre le Cancer' fellowships. P.M. is supported by a post-doctoral fellowship from the Saskatchewan Health Research Foundation.

Supplementary material available online at
http://jcs.biologists.org/lookup/suppl/doi:10.1242/jcs.110932/-/DC1

References

Abe, K., Rossman, K. L., Liu, B., Ritola, K. D., Chiang, D., Campbell, S. L., Burridge, K. and Der, C. J. (2000). Vav2 is an activator of Cdc42, Rac1, and RhoA. *J. Biol. Chem.* **275**, 10141-10149.

Antonescu, C. N., Foti, M., Sauvonnet, N. and Klip, A. (2009). Ready, set, internalize: mechanisms and regulation of GLUT4 endocytosis. *Biosci. Rep.* **29**, 1-11.

Araki, N., Johnson, M. T. and Swanson, J. A. (1996). A role for phosphoinositide 3-kinase in the completion of macropinocytosis and phagocytosis by macrophages. *J. Cell Biol.* **135**, 1249-1260.

Baldassarre, M., Pompeo, A., Beznoussenko, G., Castaldi, C., Cortellino, S., McNiven, M. A., Luini, A. and Buccione, R. (2003). Dynamin participates in focal extracellular matrix degradation by invasive cells. *Mol. Biol. Cell* **14**, 1074-1084.

Cao, H., Garcia, F. and McNiven, M. A. (1998). Differential distribution of dynamin isoforms in mammalian cells. *Mol. Biol. Cell* **9**, 2595-2609.

Chagpar, R. B., Links, P. H., Pastor, M. C., Furber, L. A., Hawrysh, A. D., Chamberlain, M. D. and Anderson, D. H. (2010). Direct positive regulation of PTEN by the p85 subunit of phosphatidylinositol 3-kinase. *Proc. Natl. Acad. Sci. USA* **107**, 5471-5476.

Chamberlain, M. D. and Anderson, D. H. (2005). Measurement of the interaction of the p85alpha subunit of phosphatidylinositol 3-kinase with Rab5. *Methods Enzymol.* **403**, 541-552.

Chamberlain, M. D., Berry, T. R., Pastor, M. C. and Anderson, D. H. (2004). The p85alpha subunit of phosphatidylinositol 3′-kinase binds to and stimulates the GTPase activity of Rab proteins. *J. Biol. Chem.* **279**, 48607-48614.

Dalle, S., Imamura, T., Rose, D. W., Worrall, D. S., Ugi, S., Hupfeld, C. J. and Olefsky, J. M. (2002). Insulin induces heterologous desensitization of G-protein-coupled receptor and insulin-like growth factor I signaling by downregulating beta-arrestin-1. *Mol. Cell. Biol.* **22**, 6272-6285.

de Chaumont, F., Dallongeville, S., Chenouard, N., Hervé, N., Pop, S., Provoost, T., Meas-Yedid, V., Pankajakshan, P., Lecomte, T., Le Montagner, Y. et al. (2012). Icy: an open bioimage informatics platform for extended reproducible research. *Nat. Methods* **9**, 690-696.

Dharmawardhane, S., Schürmann, A., Sells, M. A., Chernoff, J., Schmid, S. L. and Bokoch, G. M. (2000). Regulation of macropinocytosis by p21-activated kinase-1. *Mol. Biol. Cell* **11**, 3341-3352.

Doherty, G. J. and McMahon, H. T. (2009). Mechanisms of endocytosis. *Annu. Rev. Biochem.* **78**, 857-902.

Dufour, A., Meas-Yedid, V., Grassart, A. and Olivo-Marin, J. C. (2008). Automated quantification of cell endocytosis using active contours and wavelet. *Proceedings of the 17th International Conference on Pattern Recognition*, pp. 576-579. Los Alamos, CA: IEEE Computer Society.

Engqvist-Goldstein, A. E. and Drubin, D. G. (2003). Actin assembly and endocytosis: from yeast to mammals. *Annu. Rev. Cell Dev. Biol.* **19**, 287-332.

Fish, K. N. (2009). Total internal reflection fluorescence (TIRF) microscopy. *Current Protocols in Cytometry* (ed. J. Paul Robinson, International Society for Analytical Cytology), unit 12.18. New York, NY: John Wiley.

Folkes, A. J., Ahmadi, K., Alderton, W. K., Alix, S., Baker, S. J., Box, G., Chuckowree, I. S., Clarke, P. A., Depledge, P., Eccles, S. A. et al. (2008). The identification of 2-(1H-indazol-4-yl)-6-(4-methanesulfonyl-piperazin-1-ylmethyl)-4-morpholin-4-yl-thieno[3,2-d]pyrimidine (GDC-0941) as a potent, selective, orally bioavailable inhibitor of class I PI3 kinase for the treatment of cancer. *J. Med. Chem.* **51**, 5522-5532.

Gaffen, S. L. (2001). Signaling domains of the interleukin 2 receptor. *Cytokine* **14**, 63-77.

Gesbert, F., Sauvonnet, N. and Dautry-Varsat, A. (2004). Clathrin-lndependent endocytosis and signalling of interleukin 2 receptors IL-2R endocytosis and signalling. *Curr. Top. Microbiol. Immunol.* **286**, 119-148.

Grassart, A., Dujeancourt, A., Lazarow, P. B., Dautry-Varsat, A. and Sauvonnet, N. (2008). Clathrin-independent endocytosis used by the IL-2 receptor is regulated by Rac1, Pak1 and Pak2. *EMBO Rep.* **9**, 356-362.

Grassart, A., Meas-Yedid, V., Dufour, A., Olivo-Marin, J. C., Dautry-Varsat, A. and Sauvonnet, N. (2010). Pak1 phosphorylation enhances cortactin-N-WASP interaction in clathrin-caveolin-independent endocytosis. *Traffic* **11**, 1079-1091.

Gu, H., Maeda, H., Moon, J. J., Lord, J. D., Yoakim, M., Nelson, B. H. and Neel, B. G. (2000). New role for Shc in activation of the phosphatidylinositol 3-kinase/Akt pathway. *Mol. Cell. Biol.* **20**, 7109-7120.

Han, J., Luby-Phelps, K., Das, B., Shu, X., Xia, Y., Mosteller, R. D., Krishna, U. M., Falck, J. R., White, M. A. and Broek, D. (1998). Role of substrates and products of PI 3-kinase in regulating activation of Rac-related guanosine triphosphatases by Vav. *Science* **279**, 558-560.

Hémar, A., Lieb, M., Subtil, A., DiSanto, J. P. and Dautry-Varsat, A. (1994). Endocytosis of the β chain of interleukin-2 receptor requires neither interleukin-2 nor the γ chain. *Eur. J. Immunol.* **24**, 1951-1955.

Hémar, A., Subtil, A., Lieb, M., Morelon, E., Hellio, R. and Dautry-Varsat, A. (1995). Endocytosis of interleukin 2 receptors in human T lymphocytes: distinct intracellular localization and fate of the receptor α, β, and γ chains. *J. Cell Biol.* **129**, 55-64.

Howes, M. T., Mayor, S. and Parton, R. G. (2010). Molecules, mechanisms, and cellular roles of clathrin-independent endocytosis. *Curr. Opin. Cell Biol.* **22**, 519-527.

Huynh, K. K. and Grinstein, S. (2008). Phagocytosis: dynamin's dual role in phagosome biogenesis. *Curr. Biol.* **18**, R563-R565.

Kang, H., Schneider, H. and Rudd, C. E. (2002). Phosphatidylinositol 3-kinase p85 adaptor function in T-cells. Co-stimulation and regulation of cytokine transcription independent of associated p110. *J. Biol. Chem.* **277**, 912-921.

Kessels, M. M. and Qualmann, B. (2002). Syndapins integrate N-WASP in receptor-mediated endocytosis. *EMBO J.* **21**, 6083-6094.

King, T. R., Fang, Y., Mahon, E. S. and Anderson, D. H. (2000). Using a phage display library to identify basic residues in A-Raf required to mediate binding to the Src homology 2 domains of the p85 subunit of phosphatidylinositol 3′-kinase. *J. Biol. Chem.* **275**, 36450-36456.

Kirkham, M. and Parton, R. G. (2005). Clathrin-independent endocytosis: new insights into caveolae and non-caveolar lipid raft carriers. *Biochim. Biophys. Acta* **1745**, 273-286.

Lajoie, P. and Nabi, I. R. (2010). Lipid rafts, caveolae, and their endocytosis. *Int. Rev. Cell Mol. Biol.* **282**, 135-163.

Lamaze, C., Dujeancourt, A., Baba, T., Lo, C. G., Benmerah, A. and Dautry-Varsat, A. (2001). Interleukin 2 receptors and detergent-resistant membrane domains define a clathrin-independent endocytic pathway. *Mol. Cell* **7**, 661-671.

Le Roux, D., Le Bon, A., Dumas, A., Taleb, K., Sachse, M., Sikora, R., Julithe, M., Benmerah, A., Bismuth, G. and Niedergang, F. (2012). Antigen stored in dendritic cells after macropinocytosis is released unprocessed from late endosomes to target B cells. *Blood* **119**, 95-105.

Malecz, N., McCabe, P. C., Spaargaren, C., Qiu, R., Chuang, Y. and Symons, M. (2000). Synaptojanin 2, a novel Rac1 effector that regulates clathrin-mediated endocytosis. *Curr. Biol.* **10**, 1383-1386.

Mousavi, S. A., Malerød, L., Berg, T. and Kjeken, R. (2004). Clathrin-dependent endocytosis. *Biochem. J.* **377**, 1-16.

Nabi, I. R. and Le, P. U. (2003). Caveolae/raft-dependent endocytosis. *J. Cell Biol.* **161**, 673-677.

Patel, J. C., Hall, A. and Caron, E. (2002). Vav regulates activation of Rac but not Cdc42 during FcgammaR-mediated phagocytosis. *Mol. Biol. Cell* **13**, 1215-1226.

Raynaud, F. I., Eccles, S. A., Patel, S., Alix, S., Box, G., Chuckowree, I., Folkes, A., Gowan, S., De Haven Brandon, A., Di Stefano, F. et al. (2009). Biological properties of potent inhibitors of class I phosphatidylinositide 3-kinases: from PI-103 through PI-540, PI-620 to the oral agent GDC-0941. *Mol. Cancer Ther.* **8**, 1725-1738.

Sandvig, K., Pust, S., Skotland, T. and van Deurs, B. (2011). Clathrin-independent endocytosis: mechanisms and function. *Curr. Opin. Cell Biol.* **23**, 413-420.

Sauvonnet, N., Dujeancourt, A. and Dautry-Varsat, A. (2005). Cortactin and dynamin are required for the clathrin-independent endocytosis of gammac cytokine receptor. *J. Cell Biol.* **168**, 155-163.

Schmid, S. L., McNiven, M. A. and De Camilli, P. (1998). Dynamin and its partners: a progress report. *Curr. Opin. Cell Biol.* **10**, 504-512.

Sells, M. A., Knaus, U. G., Bagrodia, S., Ambrose, D. M., Bokoch, G. M. and Chernoff, J. (1997). Human p21-activated kinase (Pak1) regulates actin organization in mammalian cells. *Curr. Biol.* **7**, 202-210.

Subtil, A., Hémar, A. and Dautry-Varsat, A. (1994). Rapid endocytosis of interleukin 2 receptors when clathrin-coated pit endocytosis is inhibited. *J. Cell Sci.* **107**, 3461-3468.

Subtil, A., Delepierre, M. and Dautry-Varsat, A. (1997). An α-helical signal in the cytosolic domain of the interleukin 2 receptor β chain mediates sorting towards degradation after endocytosis. *J. Cell Biol.* **136**, 583-595.

Tamás, P., Solti, Z., Bauer, P., Illés, A., Sipeki, S., Bauer, A., Faragó, A., Downward, J. and Buday, L. (2003). Mechanism of epidermal growth factor regulation of Vav2, a guanine nucleotide exchange factor for Rac. *J. Biol. Chem.* **278**, 5163-5171.

Taylor, M. J., Perrais, D. and Merrifield, C. J. (2011). A high precision survey of the molecular dynamics of mammalian clathrin-mediated endocytosis. *PLoS Biol.* **9**, e1000604.

Tolias, K. F., Cantley, L. C. and Carpenter, C. L. (1995). Rho family GTPases bind to phosphoinositide kinases. *J. Biol. Chem.* **270**, 17656-17659.

Uruno, T., Liu, J., Zhang, P., Fan, Y.-x., Egile, C., Li R., Mueller, S. C. and Zhan, X. (2001). Activation of Arp2/3 complex-mediated actin polymerization by cortactin. *Nat. Cell Biol.* **3**, 259-266.

Weissman, A. M., Klausner, R. D., Rao, K. and Harford, J. B. (1986). Exposure of K562 cells to anti-receptor monoclonal antibody OKT9 results in rapid redistribution and enhanced degradation of the transferrin receptor. *J. Cell Biol.* **102**, 951-958.

Zheng, Y., Bagrodia, S. and Cerione, R. A. (1994). Activation of phosphoinositide 3-kinase activity by Cdc42Hs binding to p85. *J. Biol. Chem.* **269**, 18727-18730.